

Fluorescent Imidazolium-Based Cyclophane for Detection of Guanosine-5'-triphosphate and I⁻ in Aqueous Solution of Physiological pH

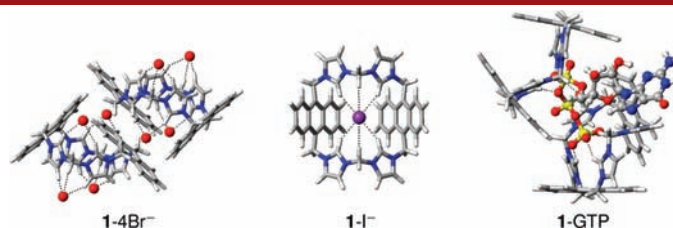
Nisar Ahmed, Bahareh Shirinfar, Inacrist Geronimo, and Kwang S. Kim*

Center for Superfunctional Materials, Department of Chemistry,
Pohang University of Science and Technology, Pohang 790-784, Korea

kim@postech.ac.kr

Received August 11, 2011

ABSTRACT



A new water-soluble and fluorescent imidazolium-anthracene cyclophane (**1**) effectively recognizes the biologically important GTP and I⁻ over other anions in a 100% aqueous solution of physiological pH 7.4. Fluorescence and ¹H NMR spectra and ab initio calculations demonstrate that emission arises from the formation of an excimer state and quenching occurs upon GTP/I⁻ binding through (C–H)⁺ · · · A⁻ hydrogen bond interactions.

The use of imidazolium-based cyclophanes has valuable applications in supramolecular chemistry and molecular recognition, particularly in sensing biologically important anionic analytes.¹ These anions include the nucleotides,

adenosine-5'-triphosphate (ATP) and guanosine-5'-triphosphate (GTP), which are fundamental units of life.² ATP is the main energy source in biological processes and plays a key role in controlling several metabolic processes and energy transduction.³ GTP acts as a substrate for the synthesis of RNA during the transcription process, provides the source of energy during metabolic reactions and protein synthesis, and plays a key role in signal transduction.⁴

(1) (a) Tabushi, I.; Yamamura, K. *Top. Curr. Chem.* **1983**, *113*, 145–185. (b) Murakami, Y. *Top. Curr. Chem.* **1983**, *115*, 107–155. (c) Murakami, Y. *J. Inclusion Phenom.* **1984**, *2*, 35–47. (d) Murakami, Y.; Kikuchi, J. *Pure Appl. Chem.* **1988**, *60*, 549–554. (e) Yoon, J.; Kim, S. K.; Singh, N. J.; Kim, K. S. *Chem. Soc. Rev.* **2006**, *35*, 355–360. (f) Chellappan, K.; Singh, N. J.; Hwang, I.-C.; Lee, J. W.; Kim, K. S. *Angew. Chem., Int. Ed.* **2005**, *44*, 2899–2903.

(2) (a) Neelakandan, P. P.; Hariharan, M.; Ramaiah, D. *J. Am. Chem. Soc.* **2006**, *128*, 11334–11335. (b) Fechter, E. J.; Olenyuk, B.; Dervan, P. B. *Angew. Chem.* **2004**, *116*, 3675–3678. (c) Fechter, E. J.; Olenyuk, B.; Dervan, P. B. *Angew. Chem., Int. Ed.* **2004**, *43*, 3591–3595. (d) Jourdan, M.; Garcia, J.; Lhomme, J.; Teulade-Fichou, M.-P.; Vigneron, J.-P.; Lehn, J.-M. *Biochemistry* **1999**, *38*, 14205–14213.

(3) Lipscomb, W. N.; Strater, N. *Chem. Rev.* **1996**, *96*, 2375–2434. (4) Alberts, B.; Johnson, A.; Lewis, J.; Raff, M.; Roberts, K.; Walter, P. *Mol. Biol. Cell*; Garland Science: New York, 2002.

(5) Ho, H. A.; Leclerc, M. *J. Am. Chem. Soc.* **2003**, *125*, 4412–4413.

(6) (a) Kim, S. K.; Singh, N. J.; Kim, S. J.; Kim, H. G.; Kim, J. K.; Lee, J. W.; Kim, K. S.; Yoon, J. *Org. Lett.* **2003**, *5*, 2083–2086. (b) Ihm, H.; Yun, S.; Kim, H. G.; Kim, J. K.; Kim, K. S. *Org. Lett.* **2002**, *4*, 2897–2900. (c) Yoon, J.; Kim, S. K.; Singh, N. J.; Lee, J. W.; Yang, Y. J.; Chellappan, K.; Kim, K. S. *J. Org. Chem.* **2004**, *69*, 581–583. (d) Zhou, Y.; Xu, Z.; Yoon, J. *Chem. Soc. Rev.* **2011**, *40*, 2222–2235. (e) Xu, Z.; Singh, N. J.; Kim, S. K.; Spring, D. R.; Kim, K. S.; Yoon, J. *Chem.—Eur. J.* **2011**, *17*, 1163–1170.

(7) (a) Bondy, C. R.; Gale, P. A.; Loeb, S. J. *J. Am. Chem. Soc.* **2004**, *126*, 5030–5031. (b) Chmielewski, M. J.; Charon, M.; Jurczak, J. *Org. Lett.* **2004**, *6*, 3501–3504. (c) Nielsen, K. A.; Jeppesen, J. O.; Levillain, E.; Becher, J. *Angew. Chem.* **2003**, *115*, 197–201. (d) *Angew. Chem., Int. Ed.* **2003**, *42*, 187–191. (e) Cho, E. J.; Moon, J. W.; Ko, S. W.; Lee, J. Y.; Kim, S. K.; Yoon, J.; Nam, K. C. *J. Am. Chem. Soc.* **2003**, *125*, 12376–12377. (f) Wallace, K. J.; Belcher, W. J.; Syed, K. F.; Seed, J. W. *J. Am. Chem. Soc.* **2003**, *125*, 9699–9715. (g) Mizuno, T.; Wei, W.-H.; Eller, L. R.; Sessler, J. L. *J. Am. Chem. Soc.* **2002**, *124*, 1134–1135. (h) Haj-Zaroubi, M.; Mitzel, N. W.; Schmidtchen, F. P. *Angew. Chem.* **2002**, *114*, 111–114. (i) Haj-Zaroubi, M.; Mitzel, N. W.; Schmidtchen, F. P. *Angew. Chem., Int. Ed.* **2002**, *41*, 104–107. (j) Schmidtchen, F. P. *Org. Lett.* **2002**, *4*, 431–434. (k) Caféo, G.; Kohnke, F. H.; La Torre, G. L.; White, A. J. P.; Williams, D. J. *Angew. Chem.* **2000**, *112*, 1556–1558. (l) Sirish, M.; Schneider, H.-J. *J. Am. Chem. Soc.* **2000**, *122*, 5881–5882. (m) Niikura, K.; Bisson, A. P.; Anslyn, E. V. *J. Chem. Soc., Perkin Trans. 2* **1999**, 1111–1114. (n) Ahmed, N.; Geronimo, I.; Hwang, I.-C.; Singh, N. J.; Kim, K. S. *Chem.—Eur. J.* **2011**, *17*, 8542–8548. (o) Kim, H. N.; Guo, Z.; Zhu, W.; Yoon, J.; Tian, H. *Chem. Soc. Rev.* **2011**, *40*, 79–93.

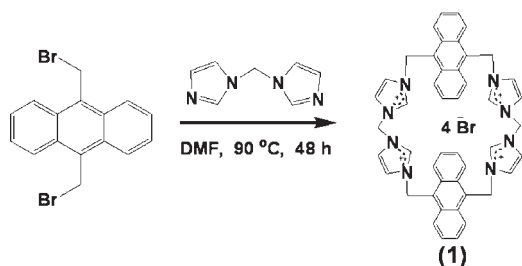
Iodide is of particular interest due to its essential role for thyroid gland function.⁵ Radioactive ¹³¹I is a component of nuclear fallout in nuclear power accidents and a particularly dangerous one due to the thyroid gland's propensity to concentrate ingested iodine.

We have studied pyridine-, benzene-, and anthracene-based receptors with imidazolium units which bind effectively with anionic species through (C–H)⁺···A[−] H-bond interactions.⁶ In contrast, anion receptors with amide, pyrrole, urea, ammonium, and guanidinium groups form N–H···A[−] H-bonds with the analyte.⁷ This presents a challenge to selective recognition of anions under physiological pH conditions due to competitive H-bonding from the solvent. Detection of ATP and GTP is further complicated by H-bonding hydroxyl groups in the sugar moiety.² The difficulty for iodide sensing arises from its large ionic radius, low charge density, and weak H-bonding ability,³ as compared to fluoride or chloride for which many sensors have been reported.⁸ An ingenious strategy is the use of fluorescent signaling subunits, such as acridine, naphthalene, pyrene, and anthracene, in the sensor. Attractive features of sensors based on anion-induced changes in fluorescence are simplicity and high sensitivity.⁹ A few examples of selective fluorescent chemosensors for ATP, GTP, and I[−] in an aqueous solution have been reported so far. The aromatic moieties of ATP and GTP form π -interactions with the signaling unit of the chemosensor and causes quenching or enhancement of fluorescence.¹⁰ On the other hand, the excellent electron donor ability of I[−] should make this anion very appropriate for sensors based on fluorescence quenching.⁸

The design and synthesis of functional cyclophanes that are soluble in aqueous media and can undergo specific interactions with biomacromolecules is quite difficult. Cyclophane sensors are more advantageous due to having a more fixed arrangement of donor atoms, as compared to a similar system containing fewer or no rings.¹¹ Thus, this would be ideal for receptors sensing GTP and I[−], and it

would be very useful to synthesize water-soluble and fluorescent imidazolium-based cyclophanes which have not been reported so far. In this regard, we report a new imidazolium-anthracene cyclophane, which not only differentiates the structurally similar GTP and ATP but also exhibits extremely high selectivity for I[−] among halides and some other anions (e.g., NO₃[−] and HSO₄[−]). The new fluorescent chemosensor, **1**, with four imidazolium units, is the first of this type of cyclophane that serves the dual function of halide and nucleotide sensor in a 100% aqueous solution through chelation-enhanced fluorescence quenching (CHEQ) of excimer emission.

Scheme 1. Synthesis of **1**



Chemosensor **1** was synthesized by the reaction of 9,10-bis(bromomethyl)anthracene with 1-(1H-imidazol-1-ylmethyl)-1H-imidazole in anhydrous DMF, followed by recrystallization from methanol with an 85% yield (Scheme 1). The receptor displays monomer ($\lambda_{em} = 427$ nm) and excimer ($\lambda_{em} = 525$ nm) fluorescence emissions when irradiated at 367 nm in aqueous solution. The excimer state arises from intermolecular π - π stacking¹² between the anthracene rings as evidenced by the variation of the excimer to monomer intensity ratio (I_{525}/I_{427}) over the concentration range 1.25–5.00 μ M (Figure S1).

Fluorescence titrations occurred in 100% aqueous solution at pH 7.4 (10 mM phosphate buffer). CHEQ is observed for pyrophosphate (PPi), ATP, CTP, TTP, UTP, and GTP, with the latter being the most significant. Visual features are shown in Figure 1a, notably the “turned off” fluorescence upon addition of GTP and the green color of **1**-ATP, which is presumably due to the 25 nm blue shift in the excimer emission. There is a slight blue shift in monomer emission for PPi and GTP, while that for CTP, TTP, UTP, and ATP is red-shifted, with the ATP being the most significant. Both ATP and GTP exhibit a greater blue shift in excimer emission as compared to CTP, TTP, and UTP (Figure 1b). The corresponding absorption spectra of **1** (Figure 1c) shows the characteristic absorption maximum at 376 nm due to the anthracene moiety. Decreased absorption is observed upon addition of PPi and GTP, and increased absorption, upon addition of CTP, TTP, UTP,

(8) (a) de Silva, A. P.; Gunaratne, H. Q. N.; Gunnlaugsson, T.; Huxley, A. J. M.; McCoy, C. P.; Radamacher, J. T.; Rice, T. E. *Chem. Rev.* **1997**, *97*, 1515–1566. (b) Beer, P. D.; Gale, P. A. *Angew. Chem., Int. Ed.* **2001**, *40*, 486–516. (c) Miyaji, H.; Sessler, J. L. *Angew. Chem., Int. Ed.* **2001**, *40*, 154–157.

(9) (a) Lee, C.-H.; Miyaji, H.; Yoon, D.-W.; Sessler, J. L. *Chem. Commun.* **2008**, *1*, 24–34. (b) Gunnlaugsson, T.; Glynn, M.; Tocci, G. M.; Kruger, P. E.; Pfeffer, F. M. *Coord. Chem. Rev.* **2006**, *250*, 3094–3117. (c) Martínez-Mañez, R.; Sancenón, F. *Chem. Rev.* **2003**, *103*, 4419–4476. (d) Callan, J. F.; de Silva, A. P.; Magri, D. C. *Tetrahedron.* **2005**, *61*, 8551–8588. (e) Zhao, J.; Fyles, T. M.; James, T. D. *Angew. Chem., Int. Ed.* **2004**, *43*, 3461–3464. (f) Gale, P. A. *Acc. Chem. Res.* **2006**, *39*, 465–475. (g) Kim, S. K.; Lee, D. H.; Hong, J.-I.; Yoon, J. *Acc. Chem. Res.* **2009**, *42*, 23–31. (h) Huang, X.; Guo, Z.; Zhu, W.; Xie, Y.; Tian, H. *Chem. Commun.* **2008**, 5143–5145. (i) Guo, Z.; Zhu, W.; Tian, H. *Macromolecules.* **2010**, *43*, 739–744.

(10) (a) Kwon, J. Y.; Singh, N. J.; Kim, H. N.; Kim, S. K.; Kim, K. S.; Yoon, J. *J. Am. Chem. Soc.* **2004**, *126*, 8892–8893. (b) Neelakandan, P. P.; Hariharan, M.; Ramaiah, D. *Org. Lett.* **2005**, *7*, 5765–5768. (d) Nair, A. K.; Neelakandan, P. P.; Ramaiah, D. *Chem. Commun.* **2009**, 6352–6354. (e) Wang, S.; Chang, Y. T. *J. Am. Chem. Soc.* **2006**, *128*, 10380–10381. (f) Malcolm, A. D. B. *Anal. Biochem.* **1977**, *77*, 532. (g) Vuojola, J.; Lamminmäki, U.; Soukka, T. *Anal. Chem.* **2009**, *81*, 5033–5038. (h) Corma, A.; Galletero, M. S.; García, H.; Palomares, E.; Rey, F. *Chem. Commun.* **2002**, 1100–1101.

(11) Lehn, J. M. *Perspectives in Coordination Chemistry*; VCHA, VCH: Basel, Weinheim, 1992; p 447.

(12) (a) Lee, E. C.; Kim, D.; Jurecka, P.; Tarakeshwar, P.; Hobza, P.; Kim, K. S. *J. Phys. Chem. A* **2007**, *111*, 3446–3457. (b) Kim, K. S.; Tarakeshwar, P.; Lee, J. Y. *Chem. Rev.* **2000**, *100*, 4145–418.

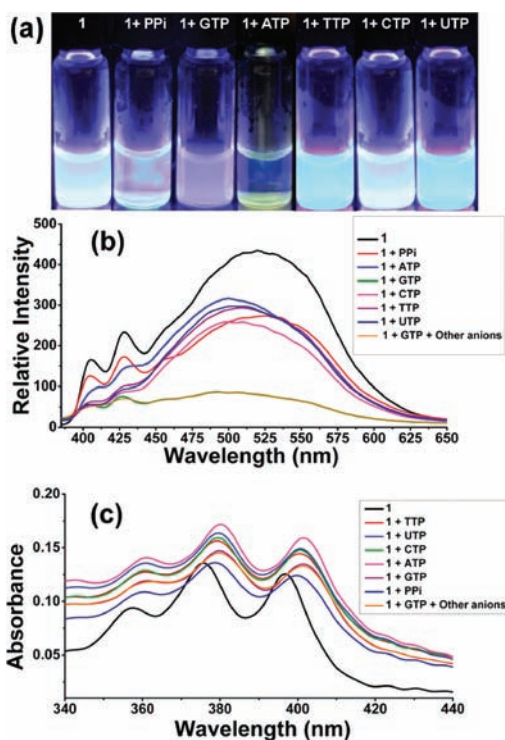


Figure 1. (a) Visual fluorescence features of **1** ($10\ \mu\text{M}$) upon the addition of sodium salts of pyrophosphate (PPI), GTP, ATP, TTP, CTP, and UTP (100 equiv) at pH 7.4 (10 mM phosphate buffer). Corresponding (b) fluorescence (slit width = 5 nm; excitation at 367 nm) and (c) absorption spectra.

and ATP. Bathochromic shifts are exhibited for PPI and GTP with isosbestic points at 398.5 and 399 nm, respectively.

The fluorescence spectra of **1** upon addition of tetrabutylammonium (TBA) salts of F^- , Cl^- , I^- , NO_3^- , and HSO_4^- (100 equiv) are shown in Figure 2a. Significant CHEQ in both monomer and excimer emission is exhibited by **1**- I^- , which can be attributed to the heavy atom effect.^{9c} The corresponding absorption spectra (Figure 2b) indicate decreased absorption with bathochromic shift. Job plot analysis indicates the formation of a 2:1 host/guest complex for GTP (Figure S2) and 1:1 complex for I^- (Figure S3). The binding constants, as determined from fluorescence titrations, are $1.1 \times 10^3/2.1 \times 10^6\ \text{M}^{-1}$ for **1**-GTP and $1.3 \times 10^4\ \text{M}^{-1}$ for **1**- I^- (Figures 3, S4, and S5). Addition of I^- up to 0.025 mM causes enhancement in monomer emission but quenching in excimer emission. However, between 0.025 and 10 mM, quenching in both monomer and excimer emissions with blue shifts of up to 2 nm is observed (Figure 3b). Detection limits were estimated (based on the criteria of fluorescence quenching) from the titration results, 4.8×10^{-7} and $8 \times 10^{-5}\ \text{M}$ for GTP and I^- , respectively.¹³

(13) Shortreed, M.; Kopelman, R.; Kuhn, M.; Hoyland, B. *Anal. Chem.* **1996**, *68*, 1414.

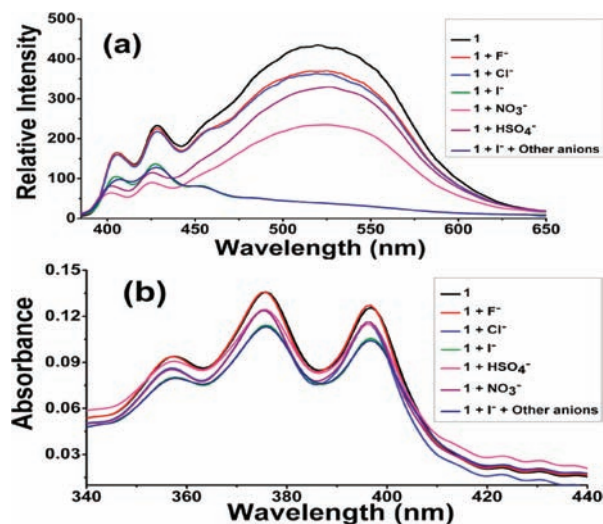


Figure 2. (a) Fluorescent emission changes of **1** ($10\ \mu\text{M}$) upon addition of TBA salts of F^- , Cl^- , Br^- , I^- , NO_3^- , and HSO_4^- (100 equiv) at pH 7.4 (10 mM phosphate buffer) (slit width = 5 nm; excitation at 367 nm). (b) Corresponding absorption spectra.

Depending on the fluorescence responses, GTP and I^- display different binding modes for receptor **1** (1:2 and 1:1, respectively). As shown in Figure S10, we postulate that two molecules of receptor **1** encapsulate GTP, with imidazolium protons interacting with the O-atoms of the phosphate groups inside the cavity. There is no interaction between anthracene moieties and guanine of GTP. The interaction of the GTP phosphate group with imidazolium protons changes the geometry of receptor **1** molecules.

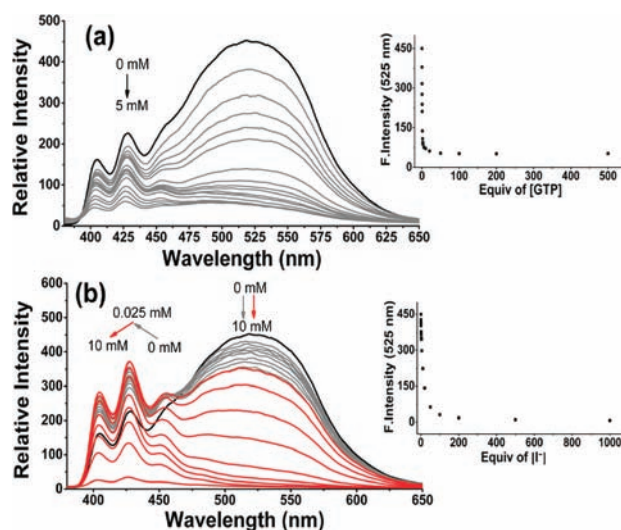


Figure 3. Fluorescence titrations of **1** ($10\ \mu\text{M}$) upon addition of (a) sodium salt of GTP and (b) TBA salts of I^- at pH 7.4 (10 mM phosphate buffer) (slit width = 5 nm; excitation at 367 nm).

The resulting separation of the face-to-face contact of anthracene units, which is a source of excimer formation, causes quenching of the excimer fluorescence. Since the emission mechanism from imidazolium to anthracene was used for communicating this binding, a significant quenching in fluorescent emission was observed in the case of GTP ions. The most stable geometry for the excimer state is depicted in Figure S10, where Br^- counteranions are situated outside the cavity and the imidazolium protons are consequently directed outward. Two molecules of receptor **1** encapsulate GTP, with imidazolium protons interacting with the O-atoms of the phosphate groups inside the cavity, and such interactions might cause the fluorescence to be turned off. Yet, I^- is bound inside the cavity in the proposed structure (**1**- I^- complex) in Figure S10 and shows a strong attraction with imidazolium protons, which may also be the reason for the separation of the face-to-face contact between anthracene units of receptor **1** molecules and quenching of the excimer fluorescence.

To gain support for the proposed binding pattern, ^1H NMR titration experiments of **1** with GTP and I^- and 2D NOESY of **1** with 1 equiv of GTP were investigated (Figures 4, S8). The ^1H NMR spectra for **1**- 4Br^- , **1**-GTP, and **1**- I^- are shown in Figure 4. Addition of 1 equiv of GTP to a 2 mM solution of **1** in $\text{DMSO-}d_6$ (Figure 4b) causes only slight (<0.1 ppm) upfield shifts of imidazolium and anthracene protons which might be due to strong binding of the phosphate group of GTP with imidazolium protons, resulting in a change of the **1**-GTP complex geometry and separation of the face-to-face interaction between anthracene units of receptor **1** molecules. The additional peak at 7.59 ppm is due to the upfield shift of the imidazolium H_d peak that can be attributed to the interaction of one imidazolium ring with the guanine moiety of GTP, resulting in an upfield shift of the H_g proton, and this interaction might also cause a change in the geometry of **1**-GTP complex. The NOE correlation between the H_g proton (with upfield shift) of GTP and imidazolium H_d (Figure S8) also revealed that the guanine moiety is located closely to one imidazolium ring. Broadening of the methylene H_f peak with an upfield shift of 0.12 ppm is observed as a result of interaction with the phosphate O-atoms as well as with the H_g proton of the guanine moiety of GTP. On the other hand, the ^1H NMR spectra for **1**- I^- indicate the $(\text{C}-\text{H})^+\cdots\text{A}^-$ ionic interaction of I^- with the protons of **1**. Upfield shifts for the imidazolium H_a (0.37 ppm) and H_c (0.66 ppm), and the anthracene H_b (0.43 ppm) peaks are significant upon addition of 1 equiv of I^- which show the strong interaction of **1** with I^- and might cause weakness and separation of the anthracene unit interaction, resulting in the **1**- I^- complex as proposed in Figure S10. Moreover, the single peak at 7.74 ppm corresponding to the anthracene H_d is split, with an upfield shift of 0.31 ppm which might be due to one side of the anthracene unit of **1** being close to I^- as compared to the other side as also proposed in the **1**- I^- complex of the figure in the Abstract and Figure S10 (Supporting Information).

The binding modes of **1**- 4Br^- , **1**-GTP, **1**- Cl^- , and **1**- I^- were determined theoretically at the PBE-D/TZV2P (def2-

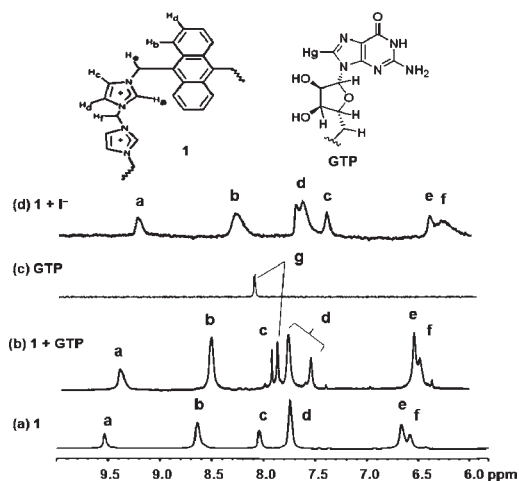


Figure 4. Partial 500 MHz ^1H NMR spectra for (a) **1** (2 mM), (b) **1**-GTP (1 equiv), (c) GTP, and (d) **1**- I^- (1 equiv). GTP and I^- were dissolved in D_2O as stock solution.

TZVPP for I) level, with aqueous solvation effects on the interaction energy incorporated using a conductor-like screening model (COSMO). The most stable geometry for the excimer state is depicted in Figure S10, where Br^- counteranions are situated outside the cavity and the imidazolium protons are consequently directed outward. The vertical separation R_v between the anthracene moieties is 3.2 Å, and the calculated interaction energy in water is -16.5 kcal/mol. Two receptor **1** molecules encapsulate GTP, with imidazolium protons interacting with the O-atoms of the phosphate groups inside the cavity at a distance of 1.7–2.1 Å. There is no interaction between the anthracene moieties and guanine of GTP, consistent with experimental ^1H NMR data. The proximity of one of the imidazole rings of **1** to the guanine moiety possibly gives rise to the additional peak observed in the ^1H NMR spectra. Yet, both Cl^- and I^- are bound inside the cavity, as evidenced by the significant upfield shifts in the ^1H NMR spectra, with calculated $(\text{C}-\text{H})^+\cdots\text{A}^-$ distances of 2.5–2.6 and 2.7–2.9 Å, respectively.

In conclusion, a new water-soluble fluorescent imidazolium anthracene receptor **1** displayed effective fluorescence quenching effects for biologically important GTP and I^- over other anions in aqueous solution of physiological pH 7.4. These affinities can be attributed to the strong $(\text{C}-\text{H})^+\cdots\text{A}^-$ ionic H-bonding.

Acknowledgment. This work was supported by NRF (National Honor Scientist Program: 2010-0020414, WCU: R32-2008-000-10180-0) and KISTI (KSC-2011-G3-02).

Supporting Information Available. Experimental procedure, compound characterization data, and theoretical calculations. This material is available free of charge via the Internet at <http://pubs.acs.org>.